Differentiation between Glioblastomas, Brain Metastases and Primary Cerebral Lymphomas using Diffusion and Perfusion Weighted Imaging

S. Wang[1], S. Kim[2], S. Chawla[1], R. L. Wolf[1], D. Knipp[1], A. Vossough[1], D. M. O'Rourke[3], K. D. Judy[3], E. R. Melhem[1], and H. Poptani[1]
[1]Radiology, University of Pennsylvania, Philadelphia, PA, United States, [2]Radiology, New York University School of Medicine, New York, NY, United States, [3]Neurosurgery, University of Pennsylvania, Philadelphia, PA, United States

Introduction

Glioblastomas, brain metastases and primary cerebral lymphomas are common brain malignancies with similar enhancement pattern on magnetic resonance (MR) imaging. Despite some characteristic MR imaging findings, it is often difficult or even impossible to differentiate these neoplasms[1]. Accurate preoperative diagnosis is crucial as the management and prognosis of these tumors are substantially different. Advanced MR techniques such as diffusion and perfusion imaging promise to increase diagnostic accuracy[2]. We have previously reported that DTI metrics including tensor shape measures can differentiate glioblastomas from brain metastases[3]. As relative cerebral blood volume (rCBV), derived from perfusion-MRI, has also been shown to correlate with tumor malignancy, we chose to evaluate whether diffusion and perfusion imaging in conjunction can be used to differentiate these three types of brain tumors.

Materials and Methods

Sixty-seven patients with histopathologic diagnosis of glioblastomas (n=26, 13M/13F, age 19-86), brain metastasis (n=25, 14M/11F, age 45-85; 18 lung, 1 melanoma, 5 breast, 1 colon) and primary cerebral lymphomas (n=16, 7M/9F, age 42-82) were included in this study. All patients underwent MR examination before surgery on a 3T Siemens Tim Trio scanner with a 12-channel phased-array head coil. DTI data was acquired using a single shot spin echo EPI sequence with parallel imaging using GRAPPA (acceleration factor = 2). Sequence parameters were as follows: TR/TE = 5000/86, NEX = 3, FOV = 22 x 22 cm^2, b = 1000 s/mm^2, number of diffusion weighting directions = 30, slice thickness 3 mm. Dynamic susceptibility contrast (DSC) T2* weighted gradient-echo echo planar images were obtained during the first pass of the standard dose of bolus injection using the following parameters: TR/TE = 2000/45, FOV = 22 × 22 cm^2, and 20 slices. Contrast-enhanced T1 weighted images, FLAIR, FA, ADC, CL, CP, CS and CBV maps were co-registered and the enhancing region of the tumor was segmented semi-automatically using IDL routines. DTI metrics as well as the rCBV values were measured from the contrast-enhancing region. A pair-wise comparison was performed for each parameter using a Mann-Whitney U test. A two level decision tree was designed to discriminate the three types of tumors. At the first level, metastases and lymphomas were grouped together as non-glioblastomas and were classified against glioblastomas. At the second level, non-glioblastomas were further sub-classified into metastases and lymphomas. At both levels, a multivariate logistic regression analysis was employed to determine the best model for classification.

Results

Boxplots of the various imaging parameters from the enhancing region of the three tumor types are shown in Fig. 1. Significantly elevated FA, CL, CP and decreased CS values were observed in glioblastomas in comparison to both brain metastases and lymphomas ($p<0.01$). ADC and rCBV values from glioblastomas were significantly higher than lymphomas. The logistic regression analysis indicated that FA [area under the curve (AUC)=0.84] was the single best predictor for classification, followed by CL (AUC=0.79) and CP (AUC=0.78). The best model to distinguish glioblastomas from non-glioblastomas consisted of FA and ADC, resulting in AUC 0.915. The result for the second level of decision tree demonstrated that the best model to differentiate lymphoma from brain metastases were comprised of ADC, CS and rCBV, resulting in AUC 0.884 (Fig.2). The overall classification result from the two levels is summarized in Table 1.

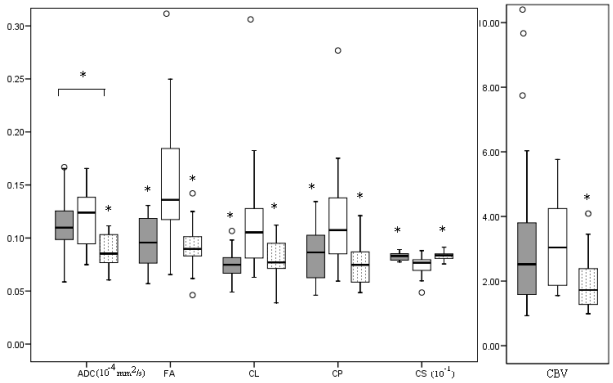

Fig. 1. Box plot of imaging characteristics in brain metastases (grey); glioblastomas (white); and primary cerebral lymphomas (dotted). The outliers were represented by circles. * indicated significant difference ($p<0.05$) for glioblastomas *vs* metastases, glioblastomas *vs* lymphomas and metastases *vs* lymphomas.

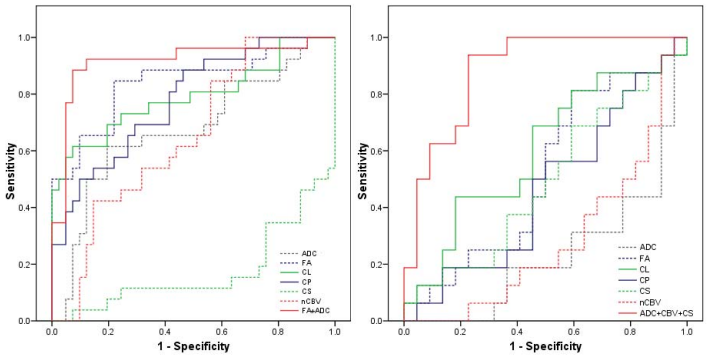

Fig 2. Receiver operative characteristic (ROC) curves from the enhancing region of the tumor. FA +ADC was the best predictor for differentiation of glioblastomas from non-glioblastomas (Left), whereas ADC+CS+CBV was the best model for distinguishing lymphomas from metastases (Right).

Table 1: Overall classification result

True Histological type	Classified as			Percentage Correct
	Glioblastomas	Metastases	Lymphomas	
Glioblastomas (n=26)	22	4		84.6
Metastases (n=25)	3	18	4	72
Lymphomas (n=16)		5	11	68.8

Discussion

The relationship between FA and tumor cellularity is controversial as both positive[4,5] and negative correlation[6] has been reported. Among tumor types studied, lymphomas usually have the highest cellularity, followed by glioblastomas and brain metastases. Elevated FA, CL, CP along with decreased CS in glioblastomas in comparison to both brain metastases and lymphomas indicates that diffusion anisotropy may not directly correlate with tumor cellularity. It has been reported that anisotropy in tumor tissue is affected by several factors including extracellular to intracellular space ratio, extracellular matrix, tortuosity, vascularity[7,8]. Individual parameters have a limited role in tumor classification. We observed that the combination of most commonly used metrics, FA and ADC from the enhancing part is the most powerful predictor to differentiate glioblastomas from other tumors. ADC combined with CS and rCBV can help distinguish lymphomas from brain metastases. Our study indicates that DTI metrics along with rCBV measurement may be helpful in tumor classification.

Reference

1. Stadnik TW, et al. Radiographics 2003;23: e7. 2. Cha S, et al. AJNR 2006; 27:475. 3. Wang S, et al. Neuroimage 2009; 44:653.
4. Kinoshita M, et al. Neuroimage 2009; 43:29. 5. Beppu T, et al. J. Neurooncol 2003; 63:109. 6. Toh CH, et al. AJNR 2008; 29:471.
7. Vargova, et al. Glia 2003; 42:77. 8. Zamecnik J, et al. Aca Neuropathol 2005; 110: 435